Inverse magnetic force microscopy of superconducting thin films

A. Badía*
Departamento de Física de la Materia Condensada, C.P.S.U.Z. - I.C.M.A., María de Luna 3, E-50.015 Zaragoza, Spain
(Received 1 May 2000; published 29 January 2001)

The recovery of the London penetration depth λ from magnetic force microscopy (MFM) data is described in the case of finite-thickness superconductors. The thickness of the superconductor b can either be treated as available data or as an additional unknown. Specifically, we show that the problem of recovering the pair (λ, b) from experimental data is well posed and we give proof of the uniqueness. No assumption is made on the symmetry of the stray field and problems with spatially extended tips of arbitrary magnetization patterns can be treated. With the inclusion of a complex penetration depth the theory is extended to *force gradient detection* modes, in which the MFM tip is oscillated at a drive frequency ω_d. For such cases, the customary methods of analysis have been revised, with the inclusion of energy transfer between the sample and the tip. We show that both the penetration depth λ and the normal fluid conductivity σ_{nf} can be recovered.

DOI: 10.1103/PhysRevB.63.094502 PACS number(s): 74.20.De, 74.25.Nf, 07.79.Pk, 02.30.−f

I. INTRODUCTION

Since the early days of superconductivity, much attention has been paid to the determination of the penetration depth λ. In particular, the temperature dependence of this quantity $\lambda(T)$ gives information on the density of superconducting electrons n_s. For instance, recall that in the London theory n_s may be operationally defined in terms of the carriers effective mass and charge as $\mu_0\lambda^2 = m_s/n_s q_s^2$. On the other hand, in the context of the BCS theory, and based on a two-fluid picture, the decrease of the superfluid density n_s with temperature results from the flow of normal fluid quasiparticles. In turn, the spectrum of these excitations strongly depends on the gap symmetry.[1] Thus, the measurement of $\lambda(T)$ allows the underlying microscopic theories to be explored. A renewed interest on such measurements has arisen with the discovery of high-T_c superconductors, for which *d*-wave pairing has been strongly suspected[2] and now seems to be convincingly established from scanning tunneling microscopy measurements.[3]

In the last decade, a new promising technique, the magnetic force microscopy[4,5] (MFM) has been applied to superconductors, which offers the advantage of probing λ within very small areas of the sample. This overcomes the difficulties associated to surface imperfections and inhomogeneities that can be hardly avoided in these materials. From the experimental point of view this technique features a more and more versatile operations.[6] However, some open questions still remain concerning the interpretation of measured data, especially in the realm of quantitative MFM (see Refs. 7 and 8 and the references therein that contain a thorough gathering of the state of the art). Essentially, it can be affirmed that one can seldomly use λ as a fit parameter for the experiments. On the contrary, due to the lack of complimentary information, one must deal with fundamental inversion procedures. In this sense, the ignorance of the magnetization function of the tip $\mathbf{M}(\mathbf{r})$ or a nonhomogeneous penetration depth $\lambda(z)$ has been already been incorporated into the theory in the aforementioned works and appropriate mathematical treatments have been devised. Nevertheless, only some simplified systems have been theoretically considered at present. In particular, recall that one must assume a *superconducting half-space* for λ to be the only intrinsic property, which can thus be determined by means of MFM. On the contrary, the available methods are questionable if other length scales are present in the problem. Along this line we should mention that a recent work[9] deals with the inverse MFM of a superconducting sphere, thus incorporating a finite size of the sample.

From the practical point of view, the very important situation of MFM for superconducting thin films still requires theoretical consideration. This case involves a magnetic tip above a superconducting slab of thickness b comparable to λ. Naturally, the magnetic force will then depend on both the scales λ and b. The topics addressed in this work will be the forward and inverse problems in such cases. In particular, we will show that one can uniquely determine λ, even in the cases in which b is an additional unknown. Moreover, a prescription on the recoverability of b from such measurements will also be given, thus allowing a nondestructive evaluation of the film thickness. Additionally, we shall focus on the analysis of *ac measurements*, for which an additional length scale is involved: the *skin depth* of normal-fluid excitations. For such measurements, we show that the customary methods of *force gradient detection modes* must be revised.

We also wish to mention that a wealth of phenomena related to the penetration depth in very thin samples[1] have been disregarded in this work. In particular, one should consider further restrictions when the thickness b shrinks to values similar to the other fundamental superconducting length ξ (coherence length). This geometrical restriction on the wave-packet size leads to a weakened superconductivity and, thus, to an increased effective penetration depth. Consequently, the present work extends the previous knowledge to the range $\xi \ll b < \lambda$, otherwise relevant in important experimental conditions.

In view of the above exposition, we can define the scope of the theory developed in this paper. Our results can be expeditiously applied to MFM experiments on type-II superconducting films in the Meissner state. To be specific, we would like to mention two systems. For the conventional NbTi one has the Ginzburg-Landau limits at zero tempera-

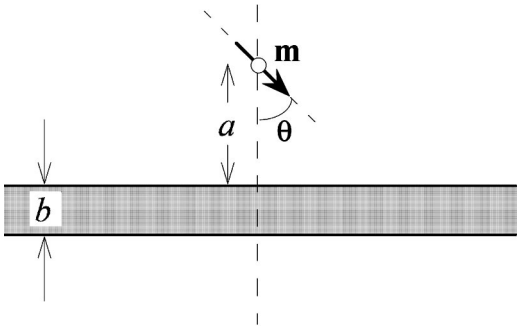

FIG. 1. Sketch of the arrangement considered in this work. A magnetic tip is placed at a distance a above a superconducting slab of thickness b. In this picture, the tip is represented by a magnetic moment $\mathbf{m}$ at an angle θ respective to the normal axis.

ture: $\lambda_{\mathrm{NbTi}}(0)=300$ nm and $\xi_{\mathrm{NbTi}}(0)=4$ nm. For the high-T_c compound YBaCuO one has in-plane values: $\lambda_{\mathrm{YBaCuO},ab}(0)=30$ nm, $\xi_{\mathrm{YBaCuO},ab}(0)=3$ nm; and along the c axis: $\lambda_{\mathrm{YBaCuO},c}(0)=200$ nm, $\xi_{\mathrm{YBaCuO},c}(0)=0.4$ nm. On the other hand, film thickness of several tens of nanometers is routinely produced.

The paper is organized as follows. Section II is devoted to the forward problem of obtaining the force between a superconducting slab and a magnetic tip of arbitrary magnetization pattern and shape. Some related topics such as the assessment of the magnetic field lines for such an arrangement are also discussed. In Sec. III we study the inversion problem of the recoverability of λ (and eventually b) from experimental data. Section IV includes the extension of the theory to force gradient detection modes (ac regime) that provide a higher experimental resolution but involve new physical phenomena. Finally, a discussion is presented (Sec. V) on the implications of this work and the realm of the previously developed *half-space geometry* models.

II. FORWARD PROBLEM

In this section we will derive expressions for the magnetic-field induction $\mathbf{B}$ arising when a magnetic tip is placed at rest above a superconducting slab of finite thickness. Magnetostatic conditions are assumed and, thus, the spatial dependence $\mathbf{B}(\mathbf{r})$ can be determined by: (i) the relation $\mathbf{B}=\mu_0\mathbf{H}$, valid for empty space and for the superconductor in the absence of demagnetizing effects, (ii) Ampère's law $\nabla\times\mathbf{H}=\mathbf{J}$, (iii) the London equations [$\mathbf{A}=-(\mu_0\lambda^2)\mathbf{J}$ in compact form], and (iv) appropriate boundary conditions at the interfaces.

First, we will concentrate on the simplified situation of a magnetic dipole at point $(0,0,a)$ above the superconductor and components (m_x,m_y,m_z) (see Fig. 1). The magnetic-field induction will be written in the customary form

$$\mathbf{B}(\mathbf{r})=\begin{cases}\mathbf{B}_1(\mathbf{r})+\mathbf{B}_2(\mathbf{r}) & z\geqslant 0,\\ \mathbf{B}_3(\mathbf{r}) & -b\leqslant z\leqslant 0,\\ \mathbf{B}_4(\mathbf{r}) & z\leqslant -b,\end{cases} \tag{1}$$

where $\mathbf{B}_1(\mathbf{r})$ is the direct contribution from the magnetic dipole, $\mathbf{B}_2(\mathbf{r})$ is the induced field above the superconductor, $\mathbf{B}_3(\mathbf{r})$ is the field penetrating inside the superconductor and $\mathbf{B}_4(\mathbf{r})$ denotes the field beyond the superconductor. Following the *scattering* picture that can be associated to this problem, analogous to some wave-function tunneling through a potential barrier, these fields will be named after *incident field* ($\mathbf{B}_1$), *reflected field* ($\mathbf{B}_2$), *penetrating field* ($\mathbf{B}_3$), and *transmitted field* ($\mathbf{B}_4$).

A. Incident field

The starting point will be the expansion of $\mathbf{B}_1(\mathbf{r})$ in terms of cylinder (Bessel) functions in order to make the symmetry properties of the stray field stand out. This can be accomplished by using the customary form for the magnetic induction outside the dipole:

$$\mathbf{B}_1=\frac{\mu_0}{4\pi}\frac{3\mathbf{n}(\mathbf{n}\cdot\mathbf{m})-\mathbf{m}}{|\mathbf{r}'|^3}, \tag{2}$$

where $\mathbf{n}$ is a unit vector in the direction of the field point $\mathbf{r}'\equiv(x,y,z-a)$, together with the identity[10]

$$\frac{1}{\sqrt{\rho^2+z^2}}=\int_0^\infty dk\, e^{-k|z|}J_0(k\rho). \tag{3}$$

Here and throughout, J_n denotes the Bessel function of nth order of the first kind.

Then, accounting for the recurrence relations of Bessel functions, one can express

$$B_{1_i}=\frac{\mu_0}{4\pi}\int_0^\infty dk\left[k^2e^{-k|a-z|}\left(\sum_j G_{ij}m_j\right)\right], \tag{4}$$

where Latin indices indicate Cartesian components and the matrix elements G_{ij} are defined as ($G_{ij}=G_{ji}$)

$$G_{11}=-\frac{1}{2}J_0(k\sqrt{x^2+y^2})+\frac{x^2-y^2}{2(x^2+y^2)}J_2(k\sqrt{x^2+y^2}),$$

$$G_{12}=\frac{xy}{x^2+y^2}J_2(k\sqrt{x^2+y^2}),$$

$$G_{13}=-\frac{x}{\sqrt{x^2+y^2}}J_1(k\sqrt{x^2+y^2}),$$

$$G_{22}=-\frac{1}{2}J_0(k\sqrt{x^2+y^2})+\frac{y^2-x^2}{2(x^2+y^2)}J_2(k\sqrt{x^2+y^2}),$$

$$G_{23}=-\frac{y}{\sqrt{x^2+y^2}}J_1(k\sqrt{x^2+y^2}),$$

$$G_{33}=J_0(k\sqrt{x^2+y^2}). \tag{5}$$

These elements have actually been obtained under the restriction $|a-z|=a-z$, which holds in the region $a>z$ where the boundary conditions will be imposed.

B. Reflected, penetrating, and transmitted fields

Next, $\mathbf{B}_2$, $\mathbf{B}_3$, and $\mathbf{B}_4$ can be determined by means of the physical laws mentioned at the beginning of this section. When combining them with the *solenoidal* character of $\mathbf{B}$, one gets the governing differential equations

$$\nabla^2\mathbf{B}_2=0,$$

$$\nabla^2\mathbf{B}_3=(1/\lambda^2)\mathbf{B}_3,$$

$$\nabla^2\mathbf{B}_4=0. \tag{6}$$

The solutions of these equations (Laplace's and Helmholtz's) can be expanded in cylindrical coordinates.[11] By comparison with the symmetry properties of the incident field, we can use the following forms for the reflected, penetrating, and transmitted fields:

$$B_{2_i}=\frac{\mu_0}{4\pi}\int_0^\infty dk\left[C_{2_{xy}}(k)e^{-k(a+z)}k^2\left(\sum_j G_{ij}m_j\right)_{i=1,2}\right], \tag{7a}$$

$$B_{2_i}=\frac{\mu_0}{4\pi}\int_0^\infty dk\left[C_{2_z}(k)e^{-k(a+z)}k^2\left(\sum_j G_{ij}m_j\right)_{i=3}\right], \tag{7b}$$

$$B_{3_i}=\frac{\mu_0}{4\pi}\int_0^\infty dk\left\{[C^+_{3_{xy}}(k)e^{\gamma z}+C^-_{3_{xy}}(k)e^{-\gamma z}]e^{-ka}k^2\left(\sum_j G_{ij}m_j\right)_{i=1,2}\right\}, \tag{7c}$$

$$B_{3_i}=\frac{\mu_0}{4\pi}\int_0^\infty dk\left\{[C^+_{3_z}(k)e^{\gamma z}+C^-_{3_z}(k)e^{-\gamma z}]e^{-ka}k^2\left(\sum_j G_{ij}m_j\right)_{i=3}\right\}, \tag{7d}$$

$$B_{4_i}=\frac{\mu_0}{4\pi}\int_0^\infty dk\left[C_{4_{xy}}(k)e^{-k(a-z-b)}k^2\left(\sum_j G_{ij}m_j\right)_{i=1,2}\right], \tag{7e}$$

$$B_{4_i}=\frac{\mu_0}{4\pi}\int_0^\infty dk\left[C_{4_z}(k)e^{-k(a-z-b)}k^2\left(\sum_j G_{ij}m_j\right)_{i=3}\right], \tag{7f}$$

where we have introduced $\gamma\equiv\sqrt{k^2+1/\lambda^2}$.

We note in passing that mathematically valid, but divergent solutions for the reflected and transmitted fields have been excluded.

The problem will be eventually closed after a brief discussion on the boundary conditions, which allow the coefficients $C(k)$ to be determined. Admissible fields $\mathbf{B}$ are particular solutions of Laplace's and Helmholtz's equations that should hold continuous components and continuous normal derivatives at the interfaces. These properties follow from the solenoidality of the field and from the finite valuedness of λ. It is simple to show that, calling on the mentioned conditions at the interfaces $(z=0, z=-b)$, one gets

$$C_{2_z}=-\Delta(\gamma^2-k^2)(1-e^{-2\gamma b}),$$

$$C^+_{3_z}=2k\Delta(\gamma+k),$$

$$C^-_{3_z}=2k\Delta(\gamma-k)e^{-2\gamma b},$$

$$C_{4_z}=4k\gamma\Delta e^{-\gamma b}, \tag{8}$$

where we have used $\Delta=1/[(\gamma+k)^2-(\gamma-k)^2e^{-2\gamma b}]$.

The coefficients C_{xy} will be determined invoking the continuity of the field and the conditions $C_{2_{xy}}=-C_{2_z}, C_{4_{xy}}=C_{4_z}$ that follow from $\nabla\cdot\mathbf{B}=0$ when comparing $\mathbf{B}_2$ and $\mathbf{B}_4$ with $\mathbf{B}_1$. Then, we obtain

$$C^+_{3_{xy}}=2\gamma\Delta(\gamma+k)$$

$$C^-_{3_{xy}}=-2\gamma\Delta(\gamma-k)e^{-2\gamma b}.$$

These results have been compared with the vector potential oriented predictions of Refs. 12 and 13. Our generalization reduces to the particular configurations considered there in the appropriate limits.

Further confirmation of the orderliness of our issue can be obtained by inspection of the predicted magnetic induction pattern under particular conditions. In regard to this, Fig. 2 displays the effect of a decreasing value of λ/b on the magnetic induction field lines when a magnetic dipole is held in the vicinity of a superconducting slab at a small angle $\theta=5°$ with respect to the normal axis. These lines have been obtained by numerical integration in a polar coordinate system and using a Runge-Kutta algorithm. Observe the continuous deformation of the dipole lobes toward a quadrupole pattern for small values of λ/b. Such a final pattern could be simulated by superimposing an image dipole to the incident field lines.

C. Magnetic force

In the approximation of a magnetic dipole tip (m_x,m_y,m_z) at point $(0,0,a)$, the self-interaction energy $U=-(1/2)\mathbf{m}\cdot\mathbf{B}_2$ allows a straightforward calculation of the vertical magnetic force $F_z=-\partial_a U$. Starting with Eqs. (7a) and (7b), and observing the limiting values of elements G_{ij} as $x,y\to 0$, we have

$$F_z=\frac{\mu_0}{8\pi}\int_0^\infty dk\, C_{2_{xy}}(k)e^{-2ak}k^3(m^2+m_z^2), \tag{9}$$

where $m^2=\Sigma_i m_i^2$. This expression is consistent with the results obtained in Ref. 12.

The generalization to problems with spatially extended tips of an arbitrary magnetization pattern follows calling on superposition. Then, using $\mathbf{M}(\mathbf{r})$ for the magnetization function and V for the volume of the tip, one gets

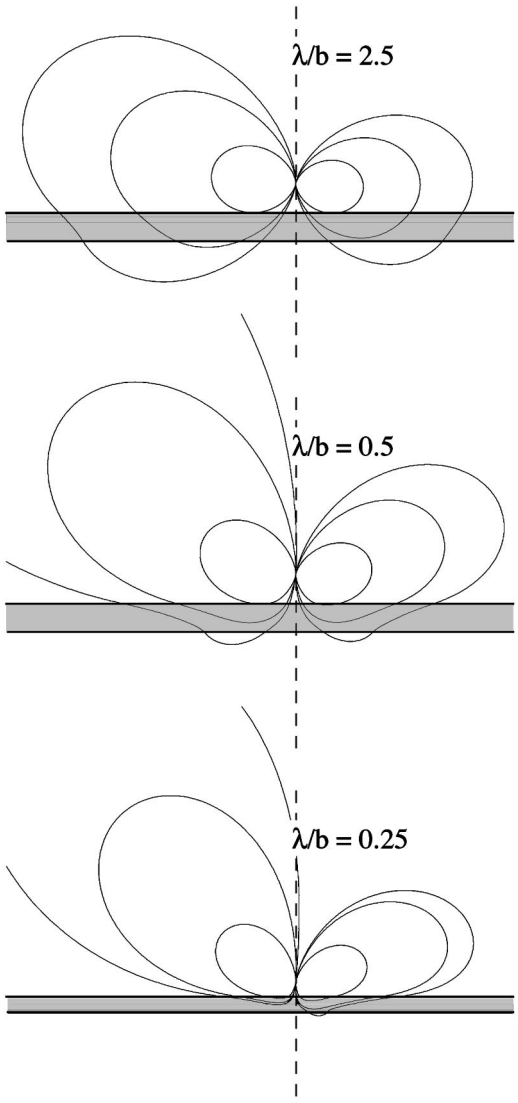

FIG. 2. Magnetic field lines for a point dipole above a superconducting slab under various conditions. In all cases, a tilt $\theta=5°$ of the magnetic moment respective to the axis has been assumed. The three panels show the field lines of **B** on the symmetry plane (defined by **m** and the axis) and have been calculated under the condition $a=b$. Notice that the case $\lambda/b=0.25$ has been scaled to 50% for clarity.

$$F_z(a)=\frac{\mu_0}{4\pi}\int_0^\infty dk\int_V d^3\mathbf{r}\int_V d^3\mathbf{r}'\left\{k^3 C_{2_{xy}}(k)e^{-2ak}e^{-k(z+z')}\times\left[\sum_{i,j} M_i(\mathbf{r})g_{ij}(\mathbf{r}-\mathbf{r}')M_j(\mathbf{r}')\right]\right\}, \tag{10}$$

where the matrix elements g_{ij} are defined as

$$g_{ij}=\begin{cases} G_{ij} & i\neq 3,\\ -G_{ij} & i=3,\end{cases}$$

and $g_{ij}(\mathbf{r}-\mathbf{r}')$ indicates that the elements must be evaluated according to Eq. (5) by replacing $x\to x-x'$ and $y\to y-y'$. Notice that volume integration must be performed with the origin of coordinates at the lower end of the magnet, which is assumed to rest at a distance a above the surface of the superconducting film.

III. INVERSE PROBLEM

Below we shall describe a method for recovering λ from the measured force in a magnetic force microscope, which relies on the Laplace transform inversion of the experimental data. This method was already applied for the case of half-space geometry.[7,8] In the present paper, special emphasis will be put on the uniqueness of the recovered λ, both for the cases in which the thickness of the superconductor is available data or one must treat it as an additional unknown. Accordingly, we will classify the problem as *scalar inversion*, if λ is the unknown, or *vector inversion* if one must solve for the pair (λ,b).

Following the ideas of Refs. 7 and 8, the starting point will be to notice that the zero penetration depth limit of force $F_0(a)$ can be written as

$$F_0(a)=\frac{\mu_0}{4\pi}\mathcal{L}\left\{\int_V d^3\mathbf{r}\int_V d^3\mathbf{r}'\left[k'^3 e^{-k'(z+z')}\times\left(\sum_{i,j} M_i(\mathbf{r})g_{ij}(\mathbf{r}-\mathbf{r}')M_j(\mathbf{r}')\right)\right]_{k/2}\right\}(a), \tag{11}$$

where the subscript $k/2$ indicates that the quantity between brackets must be evaluated at $k'=k/2$, and $\mathcal{L}$ stands for the Laplace transform operator $\mathcal{L}[f(k)](a)=\int f(k)\exp(-ak)dk$. Then, Eq. (10) admits the following expression in terms of the inverse operator $\mathcal{L}^{-1}$:

$$\mathcal{L}^{-1}[F_z(a)](k)=C_{2_{xy}}(k/2)\mathcal{L}^{-1}[F_0(a)](k). \tag{12}$$

Recalling that $C_{2_{xy}}$ depends on λ and b, one can use the previous equation in order to devise an operational relation involving these quantities and experimental or computable data. In fact,

$$C_{2_{xy}}(k/2)=\frac{\mathcal{L}^{-1}[F_z(a)](k)}{\mathcal{L}^{-1}[F_0(a)](k)}\equiv\mathcal{L}^{-1}_{F_{z/0}}(k), \tag{13}$$

and this quantity is the ratio between the actual and the limiting force inverse Laplace transforms. Next, and for further development, we rewrite $C_{2_{xy}}(k)$ in a manner that will expedite the evaluation of the superconductor finite-thickness influence. First, we define $C_\infty\equiv(\gamma-k)/(\gamma+k)$, which is the limiting value of $C_{2_{xy}}$ for $b/\lambda\to\infty$. Then, we get

$$C_{2_{xy}}(k)=C_\infty\frac{1-e^{2bk(C_\infty+1)/(C_\infty-1)}}{1-C_\infty^2 e^{2bk(C_\infty+1)/(C_\infty-1)}}. \tag{14}$$

At this point, it is instructive to inspect the properties of the inverse Laplace transforms of simulated force measurements. This is done in Fig. 3, which displays the functions $\mathcal{L}^{-1}[F_z(a)](k)$ and $\mathcal{L}^{-1}_{F_{z/0}}(k)$ for increasing values of the

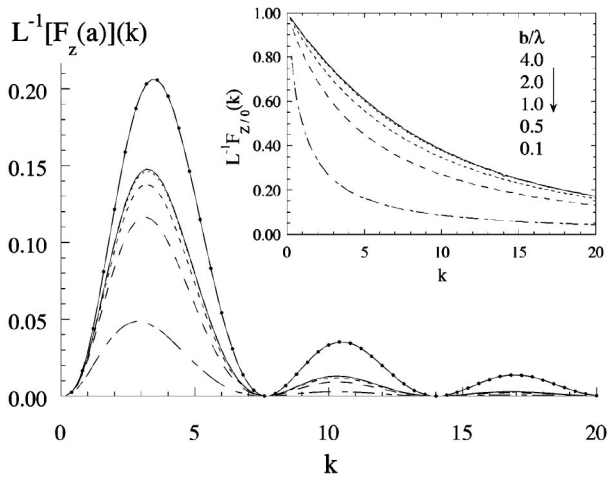

FIG. 3. Inverse Laplace transforms for simulated force versus distance measurements in the case of a cylindrical magnetic tip (radius R, length L, and $R=L\equiv D$) and $\lambda=0.1D$. The different lines correspond to various values of the ratio b/λ as shown in the inset. The dotted continuous line holds the zero penetration depth limit $\mathcal{L}^{-1}[F_0(a)](k)$ for the present geometry. In order to avoid distracting powers of 10, the normalization $\mu_0 M^2=1$ has been used. The inset shows the corresponding ratio functions $\mathcal{L}^{-1}F_{z/0}(k)$ under the same plot conventions.

ratio b/λ in the case of a cylindrical tip. It is remarkable that, for a given value of λ, a universal profile is reached as soon as $b/\lambda \gtrsim 2$. This is an assessment of the validity of the *half-space geometry* models, which remain useful even far from the limit in which they were obtained.

The question now is how to extract λ (and perhaps b) from the available information. For this purpose, it is convenient to start with the expression

$$f(k;\lambda,b)=\mathcal{L}^{-1}_{F_{z/0}}(k)-C_{2_{xy}}(k/2)=0. \tag{15}$$

Then, one must distinguish between the cases in which either λ or the pair (λ,b) is the unknown.

A. Scalar inversion

Assume, at first, that the thickness of the superconductor b can be measured by other means and therefore only λ is to be recovered from the MFM data. One can proceed as follows. (i) Consider the associated coefficient C_∞ as an unknown and solve for it $(C_{\infty,R})$ by means of the experimental data and Eq. (15) [upon substitution of $C_{2_{xy}}$ by means of Eq. (14)], and (ii) compute the recovered penetration depth as

$$\lambda_R(k)=\frac{1}{k}\frac{1-C_{\infty,R}(k/2)}{\sqrt{C_{\infty,R}(k/2)}}. \tag{16}$$

For this purpose, a numerical scheme has been tested that allows a very efficient computation of $C_{\infty,R}$ in terms of $\mathcal{L}^{-1}_{F_{z/0}}$. The algorithm relies on linear and quadratic interpolation and bisection[14] for finding the zeroes of a real function [in our case $f(k;\lambda,b)$, where k and b are given]. Typically, five function evaluations or less are enough to solve for $C_{\infty,R}$, which provides a low-cost method for computing λ with a high precision.

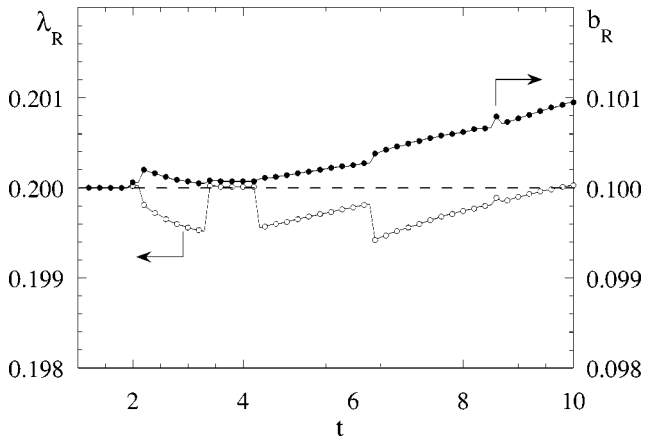

FIG. 4. Result of a vector inversion for the case of a simulated experiment with $(\lambda,b)=(0.2,0.1)$. λ_R and b_R stand for the recovered values of the penetration depth and thickness, and are plotted as a function of the wave-number ratio $t=k_2/k_1$. In this case, we have chosen $k_1=1$ (see text for details). The same cylindrical tip as in Fig. 3 was considered for the simulation.

Observe that the wave number k has been treated as a parameter in the previous paragraph. In fact, a plot of λ_R vs k is recommended in order to check for consistency.

As a concluding remark of this subsection we must mention that existence and uniqueness are guaranteed for scalar inversion. On the one hand, existence is obvious by definition of the problem, provided the physical system is described by our set of equations. On the other hand, considering λ as implicitly defined by the equation

$$f(k;\lambda,b)=0,$$

the issue of uniqueness relies on the condition

$$\frac{\partial f}{\partial \lambda}\neq 0 \quad \forall(k>0;\lambda>0,b>0),$$

which one can easily verify to hold.

Notice that, for the previous statement, we have implicitly considered that the inverse Laplace transform ratio $\mathcal{L}^{-1}_{F_{z/0}}$ is unique. In fact, this can be assumed from the physical point of view, following Lerch's theorem[11] that $\mathcal{L}^{-1}$ is specified except for a null function $N(t)$, i.e., $\int N(t)dt=0$ when integrated over *any* domain within the real positive axis.

B. Vector inversion

Here, we study the inversion process for the case of unknown penetration depth and sample thickness. As before, we assume that $\mathcal{L}^{-1}_{F_{z/0}}(k)$ is known for a collection of values of the wave number k. On choosing any couple of nontrivial values $k_1\neq k_2$, one can pose the following nonlinear system of equations:

$$\mathcal{L}^{-1}_{F_{z/0}}(k_1)-C_{2_{xy}}(k_1/2)=0,$$

$$\mathcal{L}^{-1}_{F_{z/0}}(k_2) - C_{2_{xy}}(k_2/2) = 0, \tag{17}$$

with unknowns λ and b, which become explicit when unfolding $C_{2_{xy}}$ by means of Eq. (14). For brevity, we will rewrite it in the form

$$f_1(\kappa;\lambda,b) = 0,$$

$$f_2(\kappa;\lambda,b) = 0, \tag{18}$$

where $\kappa \equiv k_1$ and $f_2(\kappa;\lambda,b) = f_1(t\,\kappa;\lambda,b)$, provided $t = k_2/k_1$. This nonlinear system has been solved numerically for faked MFM data by means of a secant algorithm.[15] The method has been tested for a variety of values for the quantities involved. As an example, Fig. 4 displays the reconstruction of λ and b for a simulated experiment. There, k_1 has been fixed and k_2 is increased by means of the parameter t (see above). It is apparent that the plot of the recovered quantities versus t is convenient to check for consistency, although a single pair (k_1,k_2) would be enough.

Finally, we want to mention that for *vector inversion*, existence is also trivial, whereas one can give proof of the uniqueness by a somewhat elaborate argument.[16]

IV. ac REGIME

It is well known that a significantly better sensitivity to long-range forces can be achieved by oscillating the flexible cantilever to which the MFM tip is attached. Specifically, one measures changes in the resonant frequency, associated to the background magnetic force.[17] Therefore, *ac operation modes* should be taken into consideration for superconducting samples. However, as we shall see below, the topic deserves an especial discussion because a number of new phenomena will occur. This was previously discussed by Coffey[18] with the coupling of all electromagnetic fields, including a normal-fluid conductivity $\sigma_{\rm nf}$ in the superconductor, and supposing the *half-space* geometry. Additionally, this was done in the linear regime, with all fields varying as $\exp(i\omega t)$ and assuming as known, constant $\sigma_{\rm nf}$. Here, we will perform a somewhat extensive analysis, with the inclusion of phase lags for the fields. Such formalism will permit a further link to the experimental quantities. In particular, we show that both λ and $\sigma_{\rm nf}$ may be recovered if one fully exploits the measurements, either in *half-space* or *finite-thickness* configurations.

It will be shown that the complete treatment of *ac* MFM of superconductors requires a restatement of conventional methods. In particular, the appearance of losses, which are usually disregarded in the *force gradient detection modes*,[5] may strongly influence the recorded signal in the case of superconductors. This topic has been fully covered for other magnetic materials and is the basis of the so-called *magnetic dissipation force microscopy* in which a reduction in the quality factor of the cantilever is detected.[19]

For the sake of clarity, we divide this section into three parts. First, we shall describe the relevant experimental details of *ac modes* and the inclusion of lossy phenomena. Then, we will concentrate on the electromagnetic field equations under steady-state conditions (forward problem). Finally, the correlation between the measured signal and the physical parameters will be established (inverse problem). Just for simplicity, this section is developed in the point dipole approximation for the magnetic tip. However, the generalization to finite-size tips in the manner of Eq. (10) is straightforward.

A. ac magnetic force microscopy with losses

The vibrational properties of force microscopy cantilevers are customary described according to the behavior of a damped harmonic oscillator. In particular, when such a system is driven by an oscillating force $F = F_0\cos(\omega_{\rm d} t)$, the tip displacement may be written as $z = A\cos(\omega_{\rm d} t - \delta)$, with the usual Lorentzian form of the amplitude

$$A = A_0 \frac{\omega_0/\omega_{\rm d}}{\sqrt{1 + Q^2(\omega_0/\omega_{\rm d} - \omega_{\rm d}/\omega_0)^2}},$$

and the phase shift given by

$$\tan\delta = \frac{1/Q}{\omega_0/\omega_{\rm d} - \omega_{\rm d}/\omega_0}.$$

Here, we have introduced the *resonance frequency* of the system ω_0 and the *quality factor* Q. Recall the relation to the *damping constant* $Q = \omega_0/\Gamma$.

Now, if one assumes that the system is driven under a simultaneous external action $\mathcal{F}$, the compliance of the cantilever will be changed, yielding modified values for the amplitude A' and phase shift δ'. Under certain conditions, one can reconstruct $\mathcal{F}$ in terms of A' and δ'. Here, we will assume small vibrations of the tip and, thus, approximate $\mathcal{F}$ as a linear function. However, as we shall see later, the inclusion of losses requires a *retarded* expression of the kind

$$\mathcal{F}(t) = Kz(t - t_{\rm r}), \tag{19}$$

where z stands for the tip's displacement in respect to equilibrium, t_r indicates the time delay, and K plays the role of a spring constant. Then, if one defines the phase lag $\varphi \equiv \omega_d t_r$, the equation of motion becomes

$$\ddot{z} + \left(\Gamma + \frac{K}{m_e}\frac{\sin\varphi}{\omega_{\rm d}}\right)\dot{z} + \left(\omega_0^2 - \frac{K}{m_e}\cos\varphi\right)z = (F_0/m_e)\cos(\omega_{\rm d} t), \tag{20}$$

where m_e is the effective mass of the cantilever. It is apparent that a steady-state vibration will occur, but with shifted resonance frequency ω_0' and damping constant Γ' (or quality factor Q'). Notice that, for the case $\varphi = 0$ (external action in phase with the tip's displacement), we get $\Gamma' = \Gamma$ and $\omega_0'^2 = \omega_0^2(1 - \partial_z\mathcal{F}/m_e\omega_0^2)$. These expressions correspond to the typical assumption in *force gradient detection modes* that the tip-sample interaction does not induce an energy transfer.

B. Forward ac problem

Thermodynamically consistent field equations for the *ac* problem can be derived by means of the *two-fluid model*,

which assumes that the full current density flowing in the superconducting state, **J**, incorporates the normal current density $\mathbf{J}_n$ maintained by unpaired electrons and the supercurrent density $\mathbf{J}_s$, so that $\mathbf{J}=\mathbf{J}_n+\mathbf{J}_s$.[1] Recall that this is a good approximation well below the energy gap frequencies ($\simeq 1$ THz). Recall also that, below such frequencies the normal-fluid conduction may be modeled by a nondispersive ohmic relation $\mathbf{J}_n=\sigma_{nf}(T)\mathbf{E}$, where the normal-fluid conductivity has been introduced. On the other hand, the combination of London equations $[\mathbf{E}=\partial_t(\mu_0\lambda^2)\mathbf{J}_s$ and $\nabla\times(\mu_0\lambda^2)\mathbf{J}_s=-\mathbf{B}]$ with Faraday's law ($\nabla\times\mathbf{E}=-\partial_t\mathbf{B}$) and Ampère's law ($\nabla\times\mathbf{B}=\mu_0\mathbf{J}$) produces the following governing equation for the magnetic field within the superconductor

$$\nabla^2\mathbf{B}=(1/\lambda^2)\mathbf{B}+\mu_0\sigma_{nf}\dot{\mathbf{B}}, \tag{21}$$

where the notation $\dot{\mathbf{B}}\equiv\partial_t\mathbf{B}$ has been introduced for brevity.

We are thus ready to solve the time-dependent problem that arises when the magnetic tip is harmonically driven. Consider a vertical vibration of the tip that can be described as a small ripple around a given tip-sample distance a, i.e., $a'=a+A'\cos(\omega_d t)$, with $A'\ll a$. In such a case, and upon replacing $a\to a'$ in Eq. (4), the time-dependent incident field components may be approximated as

$$\begin{aligned}B_{1_i}=&\frac{\mu_0}{4\pi}\int_0^\infty dk\left[k^2e^{-k(a-z)}\left(\sum_j G_{ij}m_j\right)\right]\\&-\frac{\mu_0}{4\pi}A'\cos(\omega_d t)\int_0^\infty dk\left[k^3e^{-k(a-z)}\left(\sum_j G_{ij}m_j\right)\right]\\&+\frac{\mu_0}{8\pi}A'^2\cos^2(\omega_d t)\int_0^\infty dk\left[k^4e^{-k(a-z)}\left(\sum_j G_{ij}m_j\right)\right],\end{aligned} \tag{22}$$

which we shall reexpress as

$$B_{1_i}(t)=B_{1_i}^{dc}+B_{1_i}^{\omega_d}(t)+B_{1_i}^{2\omega_d}(t),$$

indicating that the *dc* and *ac* parts of the applied field have been detached and the latter grouped in terms of their Fourier components. Notice that we must keep a second-order approximation because, eventually, a linear approximation to the force is desired.

Next, we write the reflected, penetrating, and transmitted fields as

$$B_{2_i}(t)=B_{2_i}^{dc}+B_{2_i}^{\omega_d}(t)+B_{2_i}^{2\omega_d}(t),$$

$$B_{3_i}(t)=B_{3_i}^{dc}+B_{3_i}^{\omega_d}(t)+B_{3_i}^{2\omega_d}(t),$$

$$B_{4_i}(t)=B_{4_i}^{dc}+B_{4_i}^{\omega_d}(t)+B_{4_i}^{2\omega_d}(t).$$

Hereafter, we will take advantage of the sinusoidal steady-state conditions and use the customary notation of complex numbers. Thus, we can represent the fields in the form $\mathcal{B}^*=\tilde{\mathcal{B}}\exp(i\omega t)$. The complex amplitude $\tilde{\mathcal{B}}$ allows a possible phase offset to be absorbed, which arises when one recovers the physical quantity $B^{ac}=\mathrm{Re}[\mathcal{B}^*]\equiv B_0\cos(\omega t+\Phi)$. In our case, the displacement of the tip will set the time scale reference and, thus, any phase shift will be referred to this quantity. On the other hand, ω will take the values ω_d and $2\omega_d$, corresponding to the mentioned Fourier components. Then, it is simple to verify that, on using the time-independent solutions of Sec. II B for $B_{2_i}^{dc}, B_{3_i}^{dc}$ and $B_{4_i}^{dc}$, one gets the following field equations:

$$\begin{aligned}\nabla^2\tilde{\mathbf{B}}_2^\omega&=0,\\ \nabla^2\tilde{\mathbf{B}}_3^\omega&=[1/\lambda^2+i\omega\mu_0\sigma_{nf}]\tilde{\mathbf{B}}_3^\omega,\\ \nabla^2\tilde{\mathbf{B}}_4^\omega&=0,\end{aligned} \tag{23}$$

for the complex amplitudes associated to the reflected, penetrating, and transmitted fields. This system takes the form of Eq. (6) upon defining a *complex penetration depth* through

$$\tilde{\lambda}_\omega^{-2}=\lambda^{-2}+2i\delta_{nf,\omega}^{-2},$$

where we have used the standard normal-fluid *skin depth* $\delta_{nf,\omega}\equiv\sqrt{2/\omega\mu_0\sigma_{nf}}$. Again ω can take the values ω_d and $2\omega_d$.

Next, one can impose the boundary conditions in the same manner as before (recall that they must hold for all values of t) and solve for the field components. In particular, the reflected magnetic field may be written as

$$\begin{aligned}B_{2_i}^{dc}=&\frac{\mu_0}{4\pi}\int_0^\infty dk\left[C_{2_{xy}}k^2e^{-k(a+z)}\left(\sum_j G_{ij}m_j\right)\right]\\&+\frac{\mu_0}{16\pi}A'^2\int_0^\infty dk\left[C_{2_{xy}}k^4e^{-k(a+z)}\left(\sum_j G_{ij}m_j\right)\right]\end{aligned} \tag{24}$$

and

$$\begin{aligned}\tilde{B}_{2_i}^{\omega_d}&=-\frac{\mu_0}{4\pi}A'\int_0^\infty dk\left[\tilde{C}_{2_{xy}}^{\omega_d}(k)k^3e^{-k(a+z)}\left(\sum_j G_{ij}m_j\right)\right],\\ \tilde{B}_{2_i}^{2\omega_d}&=\frac{\mu_0}{16\pi}A'^2\int_0^\infty dk\left[\tilde{C}_{2_{xy}}^{2\omega_d}(k)k^4e^{-k(a+z)}\left(\sum_j G_{ij}m_j\right)\right]\end{aligned} \tag{25}$$

for $i=1,2$. Here, $\tilde{C}_{2_{xy}}^{\omega}$ must be obtained from the *dc* counterpart by replacing $\lambda\to\tilde{\lambda}_\omega$. On the other hand, notice that, in general, a phase lag between $B_{2_i}^{ac}$ and $B_{1_i}^{ac}$ will appear.

Eventually, one can derive the time-dependent force that arises when the tip is oscillated. In fact, in the dipole limit, the instantaneous value of this quantity may be calculated as $F_z(t)=-\partial_{a'}\{-(1/2)\mathbf{m}\cdot\mathbf{B}_2[a'(t)]\}$. However, it will prove to be convenient to write it in the form $F_z(t)=F_z^{dc}+F_z^{ac}(t)$. On using the linear approximation we get

$$F_z^{dc}=\frac{\mu_0}{16\pi}\int_0^\infty dk[C_{2_{xy}}k^3e^{-2ka}(m^2+m_z^2)]$$
$$+\frac{\mu_0}{16\pi}\int_0^\infty dk[|\tilde{C}_{2_{xy}}^{\omega_d}|k^3e^{-2ka}(m^2+m_z^2)]\cos\varphi^{\omega_d} \quad (26)$$

and

$$F_z^{ac}\simeq-\frac{\mu_0}{16\pi}\int_0^\infty dk[C_{2_{xy}}k^4e^{-2ka}(m^2+m_z^2)]A'\cos(\omega_d t)$$
$$-\frac{\mu_0}{8\pi}\int_0^\infty dk[|\tilde{C}_{2_{xy}}^{\omega_d}|k^4e^{-2ka}(m^2+m_z^2)]A'\cos(\omega_d t$$
$$+\varphi^{\omega_d})-\frac{\mu_0}{16\pi}\int_0^\infty dk[|\tilde{C}_{2_{xy}}^{2\omega_d}|k^4e^{-2ka}(m^2+m_z^2)]A'$$
$$\times\cos(\omega_d t+\varphi^{2\omega_d}), \quad (27)$$

where the definition $\tilde{C}_{2_{xy}}^{\omega}\equiv|\tilde{C}_{2_{xy}}^{\omega}|\exp(i\varphi^{\omega})$ has been used. The approximation involved corresponds to considering the lowest-order correction for the incorporation of losses to the theory, i.e., taking φ^{ω} as a small parameter. Physically, this is attained if $\lambda/\delta_{\rm nf}<1$.

Notice that F_z^{dc} incorporates both the superconducting and skin depth diamagnetic terms and that one recovers Eq. (9) when the normal fluid is not present, i.e., $\varphi^{\omega_d}=0$ and $|\tilde{C}_{2_{xy}}^{\omega_d}|=C_{2_{xy}}$. Notice also that, in such case, the *ac* part of the force may be used as a linear function with effective spring constant $K=\partial_a F_z^{dc}(a)$. On the other hand, Eq. (27) may be written in the form

$$\tilde{F}_z=-\frac{\mu_0 A'}{4\pi}\int_0^\infty dk\tilde{C}_{2_{xy}}(k)e^{-2ak}k^4(m^2+m_z^2), \quad (28)$$

where we have defined

$$\tilde{C}_{2_{xy}}\equiv\frac{1}{4}C_{2_{xy}}+\frac{1}{2}\tilde{C}_{2_{xy}}^{\omega_d}+\frac{1}{4}\tilde{C}_{2_{xy}}^{2\omega_d}.$$

Eventually, the experimental quantity would be recovered as $F_z^{ac}=\mathrm{Re}[\tilde{F}_z\exp(i\omega_d t)]$, which fits the form described by Eq. (19).

C. Inverse ac problem

We shall now address the topic of recovering λ and $\sigma_{\rm nf}$ from MFM measurements in *ac* modes. First, recall that the complex amplitude of the *ac* force $\tilde{F}_z=\mathrm{Re}[\tilde{F}_z]+i\mathrm{Im}[\tilde{F}_z]$ may be experimentally solved by means of the resonance frequency and quality factor changes:

$$\frac{\mathrm{Re}[\tilde{F}_z]}{A'}=K\cos\varphi=m_e(\omega_0^2-\omega_0'^2)$$

$$\frac{\mathrm{Im}[\tilde{F}_z]}{A'}=K\sin\varphi=m_e\omega_d(\Gamma'-\Gamma).$$

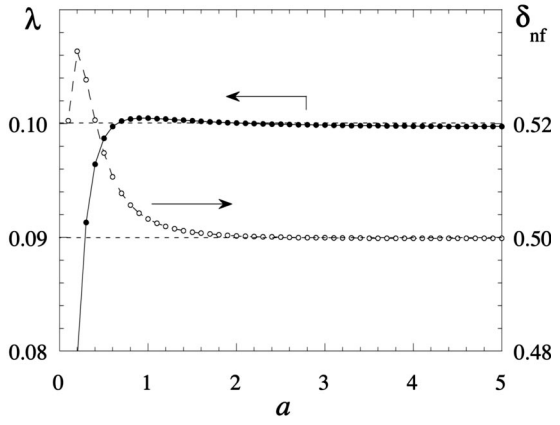

FIG. 5. Recovered penetration depth λ and skin depth $\delta_{\rm nf}$ for a simulated force versus distance experiment in *ac* operation. A point-dipole tip and half-space geometry were assumed and the complex penetration depth $\tilde{\lambda}$ was derived by means of Eq. (32). The simulation was made for $(\lambda,\delta_{\rm nf})=(0.1,0.5)$ under the normalization $\mu_0 m^2=1$

We call the reader's attention to the fact that, owing to the dissipative component of the current, the recorded force exhibits a phase lag respective to the tip's movement. Accordingly, the interpretation of *ac* modes as a measurement of the force gradient in terms of the resonant frequency shift is no longer valid. In general, one should also regard the change of the oscillator quality factor for the problem to be specified.

Several manipulations of the measured $\tilde{F}_z$ may be done in order to obtain the complex penetration depth. Essentially, they are extensions of the dc algorithms to complex variables. In order to see how it works, we include the following examples.

1. Asymptotic ac method

First, we assume a *half-space geometry* problem and apply the asymptotic theory developed in Ref. 8. In fact, the method relies on power-series reversion, which is properly defined on the complex plane. Thus, one can just follow the steps taken there. For the sake of simplicity, suppose a point dipole tip along the normal axis, i.e., $\mathbf{m}=(0,0,m)$. Then, Eq. (28) leads to

$$\tilde{f}_z\equiv\frac{\tilde{F}_z}{A'}=-\frac{\mu_0 m^2}{2\pi}\int_0^\infty dk[\tilde{C}_\infty(k)k^4e^{-2ak}], \quad (29)$$

where we have used $\tilde{C}_\infty$ for the half-space approximation of $\tilde{C}_{2_{xy}}$. Actually, this factor is the superposition of three terms $\tilde{C}_\infty=C_\infty/4+\tilde{C}_\infty^{\omega_d}/2+\tilde{C}_\infty^{2\omega_d}/4$. Associated to each term, one can develop an asymptotic series approach as in the mentioned reference. On gathering them we obtain the series expansion

$$\tilde{f}_z=F_0'+\frac{1}{4}\sum_{n=1}^{\infty}\left(-\frac{1}{2}\right)^n\alpha_n\frac{d^nF_0'}{da^n}(\lambda^n+2\tilde{\lambda}_{\omega_d}^n+\tilde{\lambda}_{2\omega_d}^n). \quad (30)$$

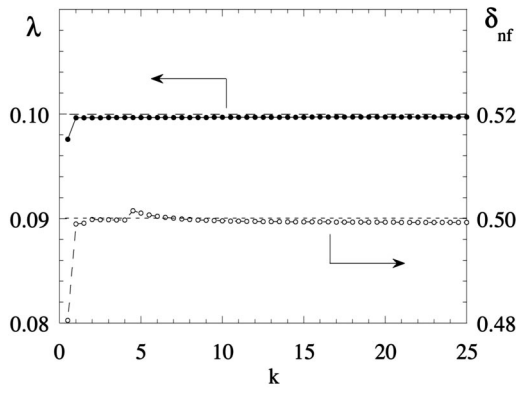

FIG. 6. Recovered penetration depth λ and skin depth $\delta_{\rm nf}$ in a simulated *ac* MFM experiment with an oscillating dipole tip over a finite-thickness superconductor ($b=0.3$). The simulation was made for $(\lambda,\delta_{\rm nf})=(0.1,0.5)$ under the normalization $\mu_0 m^2=1$. λ and $\delta_{\rm nf}$ are plotted versus the wave number k and have been obtained by means of Eq. (35).

Here, $F_0'(a)$ stands for the derivative of the perfect screening limit of the *dc* force and α_n is a numerical coefficient.[8] Next, we introduce the complex penetration depth $\tilde{\lambda}$:

$$\tilde{\lambda}\equiv\lambda[1-i(\lambda/\delta_{{\rm nf},\omega_{\rm d}})^2],$$

in terms of which

$$\tilde{f}_z\simeq F_0'+\sum_{n=1}^{\infty}\left(-\frac{1}{2}\right)^n\alpha_n\frac{d^nF_0'}{da^n}\tilde{\lambda}^n. \tag{31}$$

It is apparent that one can get $\tilde{\lambda}$ from the inverse series

$$\tilde{\lambda}=\sum_{n=1}^{\infty}\tilde{c}_n(\tilde{f}_z-F_0')^n, \tag{32}$$

where the coefficients $\tilde{c}_n$ may be obtained from their *dc* counterpart[8] just by replacing $F_0^{(n)}\rightarrow F_0^{(n+1)}$.

The asymptotic nature of the method for complex values $\tilde{\lambda}$ is illustrated in Fig. 5. We display the recovered penetration depth λ and skin depth $\delta_{\rm nf}$ from a simulated experiment in which synthetic values of $\tilde{f}_z(a)$ were obtained by means of Eq. (29). The inverse series was approximated with five terms. Notice that the approximation $\lambda^n+2\tilde{\lambda}_{\omega_{\rm d}}^n+\tilde{\lambda}_{2\omega_{\rm d}}^n\simeq\tilde{\lambda}^n$ produces a tiny reduction in the recovered values for the case $\lambda/\delta_{\rm nf}=0.2$.

2. Laplace inversion ac method: finite-thickness superconductors

To close this section, we address the problem of finite-thickness superconductors in the *ac* regime. It will be shown that a straightforward extension of the *scalar inversion* method to complex variables can be established.

Assume a situation in which the sample thickness b cannot be neglected but is available. Let us also restrict this (without loss of generality) to the case of a point-dipole tip $(0,0,m)$. Then, from Eq. (28) one gets

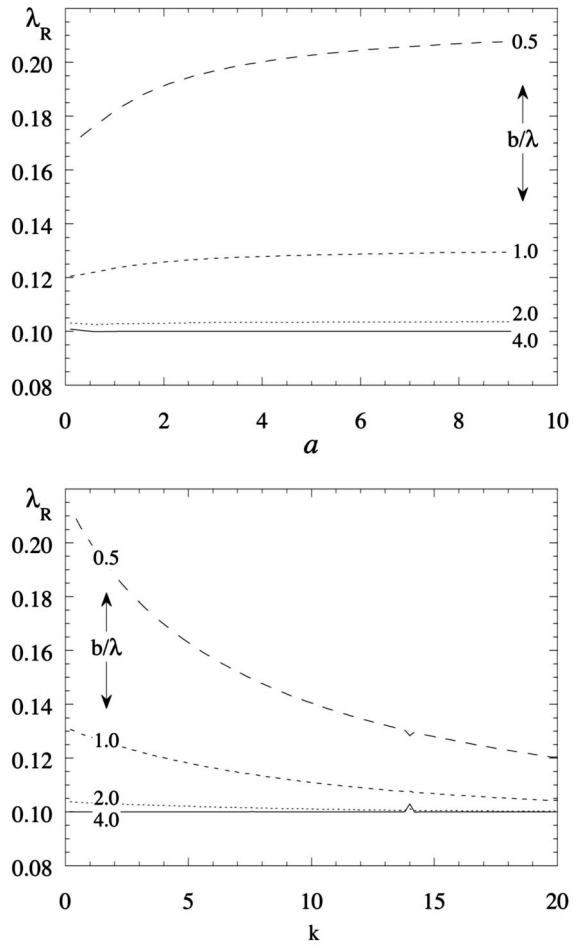

FIG. 7. Recovered penetration depth $\lambda_{\rm R}$ by means of *half-space geometry* models for simulated force versus distance experiments in the case of a cylindrical tip above superconducting slabs of various relative thickness b/λ. The upper panel displays the results for the *asymptotic* theory as a function of the recording distance for a truncated inverse series of three terms (see text). The lower panel corresponds to the *Laplace inversion* method and $\lambda_{\rm R}$ is plotted against the wave number k (see text).

$$\tilde{f}_z=-\frac{\mu_0 m^2}{64\pi}\mathcal{L}[k^4\tilde{C}_{2_{xy}}(k/2)](a), \tag{33}$$

whence

$$\tilde{C}_{2_{xy}}(k/2)=-\frac{64\pi}{\mu_0 m^2 k^4}\mathcal{L}^{-1}[\tilde{f}_z(a)](k). \tag{34}$$

This equation may be used to solve for λ and $\delta_{\rm nf}$. The quantity $\tilde{f}_z$ is supposed to be available from experimental data. Next, one can calculate the associated value $\tilde{C}_\infty(k/2)$ from

$$\tilde{C}_\infty\frac{1-e^{bk(\tilde{C}_\infty+1)/(\tilde{C}_\infty-1)}}{1-\tilde{C}_\infty^2 e^{bk(\tilde{C}_\infty+1)/(\tilde{C}_\infty-1)}}+\frac{64\pi}{\mu_0 m^2 k^4}\mathcal{L}^{-1}[\tilde{f}_z](k)=0, \tag{35}$$

which is analogous to Eq. (15) for the *dc* counterpart. If we assume again that $\lambda/\delta_{nf}<1$, the complex function $\tilde{C}_\infty$ is related to C_∞ by the substitution $\lambda\rightarrow\tilde{\lambda}$.

Eventually, we are led to the problem of finding the zeroes of a transcendental complex equation. This process has been explored for simulated experiments in which $\tilde{f}_z$ was obtained by means of Eq. (28). We have implemented Müller's method,[20] which was originally developed for polynomials but is also used for finding complex zeroes of analytic functions. To assess the method we include Fig. 6, in which the recovered values of λ and δ_{nf} are plotted versus the wave number k. As in the previous subsection, the use of the approximate complex penetration depth dependence produces a small reduction in the recovered values.

V. DISCUSSION AND CONCLUSIONS

Throughout this work we have described the progress made in the theory for recovering fundamental lengths of superconductivity by means of magnetic force microscopy. The main issues have been (i) the inclusion of the thickness of the sample b in the problem of the recovery of the penetration depth λ and (ii) the revision of the standard *force gradient detection* modes so as to recover λ and the normal-fluid *skin depth* δ_{nf} in *ac* measurements.

Regarding the topic of the finite thickness influence, we have introduced the so-called *scalar* and *vector* inversion methods, in which either λ or the pair (λ,b) are unknown. However, this problem deserves some further discussion, which can be stated as the following question: How much information can one extract from MFM measurements about the pair (λ,b)?

As it was previously discussed, the quantitative behavior of force data (and the associated Laplace transforms) is controlled by the parameter b/λ. In fact, force data merge as soon as $b/\lambda\gtrsim 2$ provided the remaining length scales are fixed. Thus, one should expect that the recovered penetration depth by means of *half-space geometry* models can be trusted if this condition is satisfied, while any information about the film thickness is simultaneously lost. In order to verify this statement, we have performed the inversion of simulated data by blindly using the *asymptotic*[8] and *Laplace inversion*[7] techniques, despite a finite value of b/λ. Typical results are shown in Fig. 7 for both approximate methods. This figure permits an answer to be given to the question made above. If one faces the problem of full ignorance about the pair (λ,b), the application of *half-space geometry* models can be used as a first test on the relative value of b/λ. A nonconstant value of the recovered penetration depth λ_R as a function of the recording distance a (even when augmenting the number of terms in the series expansion) and as a function of the wave number k indicates an inconsistent hypothesis, and a vector inversion with initial guess according to $b<2\lambda$ should be tried. On the contrary, if one finds constant and equal values of λ_R by means of the *asymptotic* and *Laplace inversion* approximations, these can be trusted, but the knowledge of b is limited to the condition $b>2\lambda_R$.

Even for the simplest case of scalar inversion, intricate transcendental equations must be solved in order to recover λ from the experimental data. Thus, several numerical schemes have been explored, which produce efficient calculations. In order to assess the convergence to the right physical solution, we give proof of the uniqueness for the involved inversion problem.

Section IV has been dedicated to the *ac* regime. First, we have shown that the standard interpretation of *ac* modes in MFM must be revised. In particular, we show that energy losses can be incorporated to the theory. These losses are naturally included as a phase lag between the tip-sample repulsion force and the displacement of the tip. Then, besides a modified resonance frequency, we predict a quality factor shift, which can be experimentally solved and λ and δ_{nf} can be obtained from the measurements. In fact, several simulations have been included in which we show that the correct values may be recovered under the assumption $\lambda<\delta_{nf}$, typically valid unless for temperatures extremely close to T_c.

Finally, we want to emphasize that all these advances in the theory of inverse MFM are straightforwardly implemented regardless of the symmetry of the stray field, i.e., an arbitrary magnetization pattern $\mathbf{M}(\mathbf{r})$ over any tip geometry is allowed, though one must not know the details of this function for the inversion procedure. In fact, the zero penetration depth limit of the repulsion force $F_0(a)$ may be used as a calibration function, which can be obtained by complimentary experiments.

ACKNOWLEDGMENT

The author acknowledges financial support from Spanish CICYT under Project No. MAT99-1028.

*Electronic address: anabadia@posta.unizar.es

[1] M. Tinkham, *Introduction to Superconductivity* (McGraw-Hill, New York, 1996), 2nd ed.

[2] W.N. Hardy, D.A. Bonn, D.C. Morgan, R. Liang, and K. Zhang, Phys. Rev. Lett. **70**, 3999 (1993); J.E. Sonier, R.F. Kiefl, J.H. Brewer, D.A. Bonn, J.F. Carolan, K.H. Chow, P. Dosanjh, W.N. Hardy, Ruixing Liang, W.A. MacFarlane, P. Mendels, G.D. Morris, T.M. Riseman, and J.W. Schneider, *ibid.* **72**, 744 (1994).

[3] S.H. Pan, E.W. Hudson, K.M. Lang, H. Eisaki, S. Uchida, and J.C. Davis, Nature (London) **403**, 746 (2000).

[4] Y. Martin and H.K. Wickramasinghe, Appl. Phys. Lett. **50**, 1455 (1987).

[5] Y. Martin, C.C. Williams, and H.K. Wickramasinghe, J. Appl. Phys. **61**, 4723 (1987).

[6] H.J. Hug, B. Stiefel, P.J.A. Vanschendel, A. Moser, S. Martin, and H.J. Guntherodt Rev. Sci. Instrum. **70**, 3625 (1999).

[7] M.W. Coffey, Phys. Rev. B **52**, 9851 (1995); **57**, 11 648 (1998); Phys. Rev. Lett. **83**, 1648 (1999); J. Appl. Phys. **87**, 392 (2000).

[8] A. Badía, Phys. Rev. B **60**, 10 436 (1999).

[9] M.W. Coffey, Inverse Probl. **15**, 669 (1999).

[10] I. S. Gradshtein and I. M. Ryzhik, *Tables of Integrals, Series, and Products* (Academic, New York, 1994).

[11] G. Arfken and H. J. Weber, in *Mathematical Methods for Physicists* (Academic, Boston, 1995), 4th ed.

[12] Z.J. Yang, Jpn. J. Appl. Phys., Part 2 **31**, L938 (1992).
[13] J.C. Wei, J.L. Chen, L. Horng, and T.J. Yang, Physica C **267**, 345 (1996).
[14] R.P. Brent, Comput. J. (UK) **14**, 422 (1971).
[15] J. E. Dennis, Jr. and R. B. Schnabel, *Numerical Methods for Unconstrained Optimization and Nonlinear Equations* (Prentice-Hall, Englewood Cliffs, NJ, 1983).
[16] In order to show that Eq. (18) has a unique solution (λ,b), one can make use of the celebrated *implicit function theorem* of differential calculus. Uniqueness is globally ensured by the condition $\partial_k[\partial_\lambda f(k,\lambda,b)/\partial_b f(k,\lambda,b)]\neq 0$. In fact, one can see that this quantity is strictly positive for all $(\kappa;\lambda_0,b_0)\in\mathbb{R}^+\times\mathbb{R}^{2+}$.
[17] P. Grütter, H. J. Mamin, and D. Rugar, in *Scanning Tunneling Microscopy II*, edited by R. Wiesendanger and H.-J. Güntherodt (Springer, Berlin, 1995), 2nd ed.
[18] M.W. Coffey, J. Supercond. **10**, 567 (1997).
[19] Y. Liu and P. Grütter, J. Appl. Phys. **83**, 7333 (1998).
[20] D.E. Müller, Math. Tables Aids Comput. **10**, 208 (1956).